

Article

Corrosion Study and Intermetallics Formation in Gold and Copper Wire Bonding in Microelectronics Packaging

Chwee Sim Goh ^{1,*}, Wee Ling Eddy Chong ¹, Teck Kheng Lee ¹ and Christopher Breach ²

¹ Institute of Technical Education, 2 Ang Mo Kio Drive, 567720, Singapore;

E-Mails: eddy_w_l_chong@ite.edu.sg (W.L.E.C.); lee_teck_kheng@ite.edu.sg (T.K.L.)

² Promat Consultants, 160 Lentor Loop, #08-05, Tower 6, 789094, Singapore;

E-Mail: cbreach@promat-consulting.com

* Author to whom correspondence should be addressed; E-Mail: goh_chwee_sim@ite.edu.sg;

Tel.: +65-68797891; Fax: +65-65805020.

Received: 8 May 2013; in revised form: 31 May 2013 / Accepted: 2 July 2013 /

Published: 17 July 2013

Abstract: A comparison study on the reliability of gold (Au) and copper (Cu) wire bonding is conducted to determine their corrosion and oxidation behavior in different environmental conditions. The corrosion and oxidation behaviors of Au and Cu wire bonding are determined through soaking in sodium chloride (NaCl) solution and high temperature storage (HTS) at 175 °C, 200 °C and 225 °C. Galvanic corrosion is more intense in Cu wire bonding as compared to Au wire bonding in NaCl solution due to the minimal formation of intermetallics in the former. At all three HTS annealing temperatures, the rate of Cu-Al intermetallic formation is found to be three to five times slower than Au-Al intermetallics. The faster intermetallic growth rate and lower activation energy found in this work for both Au/Al and Cu/Al as compared to literature could be due to the thicker Al pad metallization which removed the rate-determining step in previous studies due to deficit in Al material.

Keywords: intermetallics; reliability; wire bonding; gold; copper

1. Introduction

Au wire thermosonic bonding has been a mainstream semiconductor packaging process for many decades [1]. The inert properties of Au make it an excellent choice for use when reliable manufacturing and applications in microelectronics packaging are required. The steep increase in Au prices has triggered the demand for high volume wire bonding process that can utilize Cu wire [2]. Barriers need to be overcome in Cu wire bonding due to the high oxidation rate and hardness of Cu wires. A number of studies have been conducted on Cu wire bonding [3–6] and the expected benefits of Cu wire over Au wire have been published [7–9]. The main benefits of using Cu wire bonding over Au wire bonding are lower material cost, higher electrical and thermal conductivity, and in long period HTS conditions, the lower reaction rates between Cu and Al serves to improve the long term reliability performance.

Although the many benefits of using Cu wire have been highlighted, and the Cu wire interconnect technology is already at the stage of mass manufacturing, cracking of the wire bond interface is often reported as a result of humidity or temperature effect [10,11]. Reports have also shown the poorer reliability of Cu as compared to Au in the presence of halides in conventional mold compounds and encapsulant materials [12]. The corrosion cell initiates due to the difference in electrochemical potential between Al and Cu in the presence of an electrolyte. The self-passivation of Cu worsens in an acidic environment where the Cl^- ions in mold compounds act as a catalyst in the presence of moisture. This increases the corrosion rate of Cu by making the ranges of stable pH for Cu much narrower. Although the individual intermetallic phases that will corrode have been predicted in the previous study, microstructural evidence has not been reported to account for the corrosion behavior. The behavior of Au in halide environment has not been reported widely as the former has been esteemed as a noble metal. However, the potential difference between the Au wire and Al pad may pose an issue which can lead to severe galvanic corrosion in the Al pad, and subsequently to Au ball detachment.

The intermetallic growth mechanisms of Cu on Al pad metallization has been studied by a few researchers [2,3,6]. The activation energy reported varies from a wide range of 10.71 kJ/mol to 60.9 kJ/mol. The thin Al metallization could be an important factor in affecting the rate of formation of Cu-Al intermetallics due to the limiting material effect. The intermetallic growth mechanisms of Au on Al pad has been reported to a much lesser extent [3], and the activation energy of Au has not been widely published.

Accordingly, to address the shortfall in the corrosion studies conducted in halide environment, and the intermetallic growth mechanisms of Au and Cu, this paper focuses on these two aspects in Au/Al and Cu/Al wire bonding. Comparison studies between Au/Al and Cu/Al will be carried out to examine the difference in their corrosion behaviors and intermetallics formation.

2. Experimental

2.1. Bonding Parameters and Material Properties of Au and Cu wires

The Au and Cu wires were bonded to the Al/0.5% Cu pad of 1.2 μm thickness using the ASM Eagle 60AP wire bonder. Tables 1 and 2 show the material properties of Au and Cu wires, and the bonding parameters used respectively. The number of bonded wires per sample is 100.

Table 1. Material properties of Au and Cu wires.

Property	Au	Cu
Composition	99.99% Au	99.99% Cu
Diameter (μm)	25	25
Specified Breaking Load (g)	9.7~17.4	6.8~14.5
Elongation (%)	2~7	6~18

Table 2. Wire bonding parameters.

Parameter	Au	Cu
Bonding Time (ms)	10.0	9.0
Bonding Force (gf)	26.0	9.0
Ultrasonic Power (mW)	256	306

2.2. Corrosion Studies in Halide Environment

For corrosion studies in Cl^- environment, 10 dummy dies and 10 non-encapsulated dummy dies with Au and Cu wire bonds were soaked in random solutions of 0.1 M, 0.01 M and 0.001 M of NaCl solutions. Through macroscopic analysis of the samples that have been soaked in the three solutions, it was observed that a significant number of bonded Au and Cu balls were detached from the bond pads. Comparison of the corrosion behaviors of Au and Cu ball bonds was not possible as most of the bonded balls were detached.

To give a more representative composition of Cl^- in the actual operating environment, the content of Cl^- in halogen-free mold compound was estimated. 500 ppm Cl^- content was used as a guideline to compute the NaCl concentration for the test. An estimated concentration of 8.56×10^{-3} M of NaCl was computed for 500 ppm Cl^- based on the diffusion coefficient of polymeric materials. Dummy dies and non-encapsulated Au and Cu wire bonded dies were soaked at 25 $^\circ\text{C}$, and microscopic examination was conducted at 0, 5, 10, 15, 20, 25 and 30 min interval. The number of wires examined is 240 per time interval.

2.3. Intermetallic Growth Rate Evaluation in Au/Al and Cu/Al Wire Bonding

The Au/Al and Cu/Al wire bonding samples were placed in the air convection oven at 175 $^\circ\text{C}$, 200 $^\circ\text{C}$ and 225 $^\circ\text{C}$ for 120, 240, 360 and 480 h respectively. Table 3 shows the specific high temperature storage (HTS) conditions for intermetallic growth.

Table 3. High temperature storage conditions for intermetallic growth.

Condition	Temperature (°C)		
	175	200	225
Duration (h)	120	120	120
	240	240	240
	360	360	360
	480	480	480

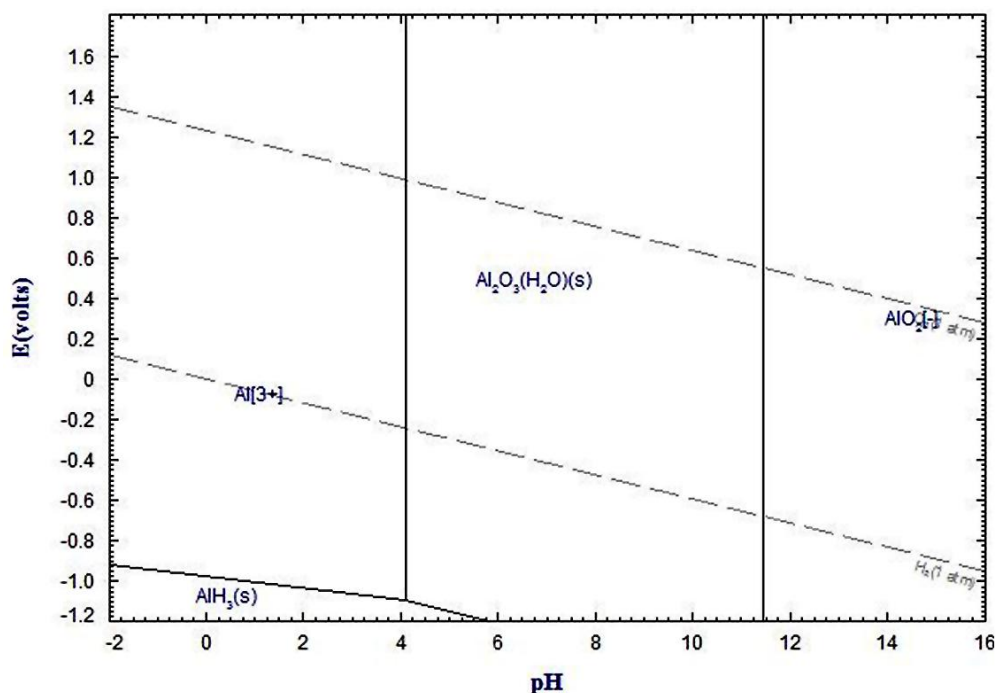
After completion of high temperature storage at each condition, the Au/Al and Cu/Al wire bonding samples were epoxy mounted, grinded and polished to 1 μm finishing. Subsequently, the samples were ion polished using the JEOL IB-09010CP cross section polisher. The intermetallic thickness in Au/Al and Cu/Al samples were then analyzed using the JEOL JSM-7600F field emission scanning electron microscope (FESEM) in the LaBeTM. Low energy backscatter imaging mode to show a good contrast in the intermetallic layers and parent material. The intermetallic thickness is taken from an average of 10 measurements of three wire balls per sample.

3. Results and Discussion

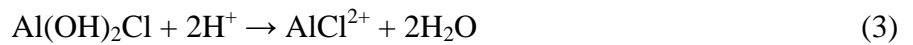
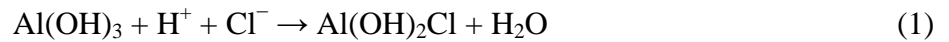
3.1. Corrosion Studies in Halide Environment

In the presence of dissolved CO_2 in the 8.56×10^{-3} M of NaCl in deionized water, the pH of the solution is about 5.0. According to Al Pourbaix diagram at 25 °C [13] as shown in Figure 1, a passivation layer is formed according to $\text{Al}_2\text{O}_3 + 3\text{H}_2\text{O} \rightarrow 2\text{Al}(\text{OH})_3$.

Figure 1. Pourbaix or potential-pH diagram of Al in aqueous environment, calculated for a temperature of 300 K and a molality of 1e^{-6} mol/kg [13].

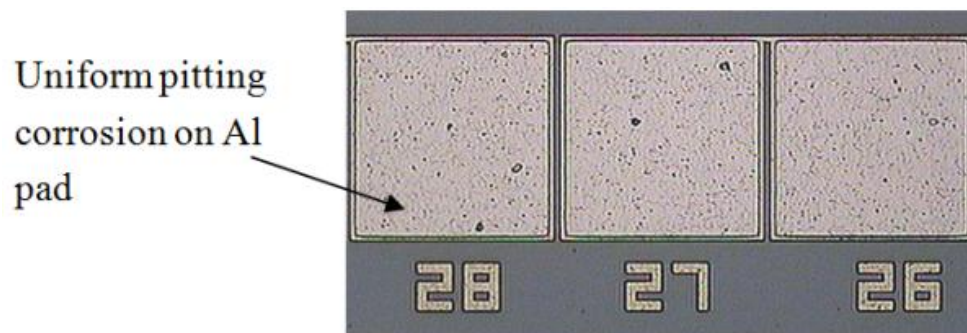


In the presence of Cl^- in the slightly acidic deionized water, the following corrosion reactions are expected to take place on the Al bond pads [14]:



Uniform pitting corrosion on the Al pads will take place in the slightly acidic halide environment according to Equations (1) to (3), and this is shown in the dummy dies without any wire bonding in Figure 2.

Figure 2. Uniform pitting corrosion on Al pads occurring on the dummy dies without any wire bonding.



In addition to pitting corrosion on the Al pads, galvanic corrosion due to the presence of Au or Cu balls bonded on the pads can also take place. This is due to the electrode potential difference between Au or Cu and Al. Figure 3 shows the mechanism of galvanic corrosion between the Au balls and Al pads. The Au balls in Figure 3a,b were still intact after 30 min of soaking in NaCl solution in the initiation and propagation stages, and were sheared off to reveal the state of corrosion beneath the balls. Figure 3c shows that corrosion has spread to the whole bonded area beneath the Au ball and the ball is detached without shearing.

Figure 3. Corrosion mechanism of Au balls and Al pad at the (a) initiation stage; (b) propagation stage and (c) detachment stage.

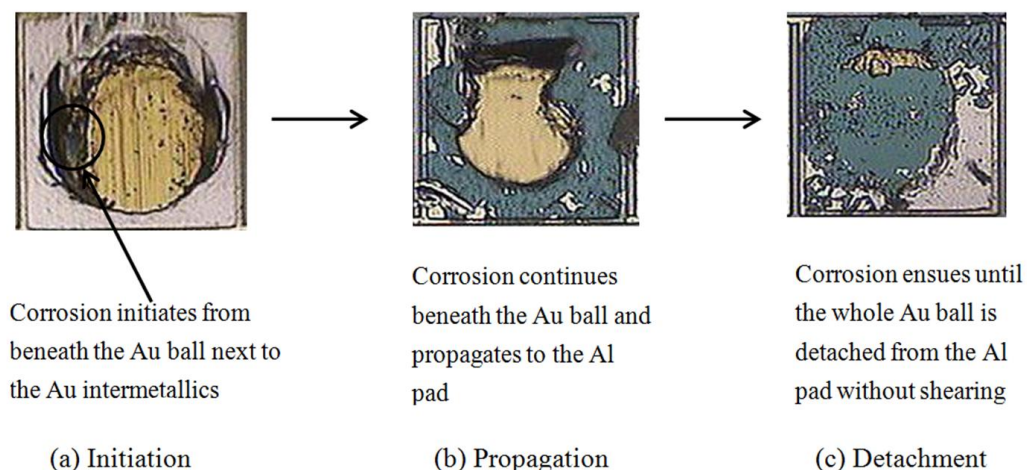
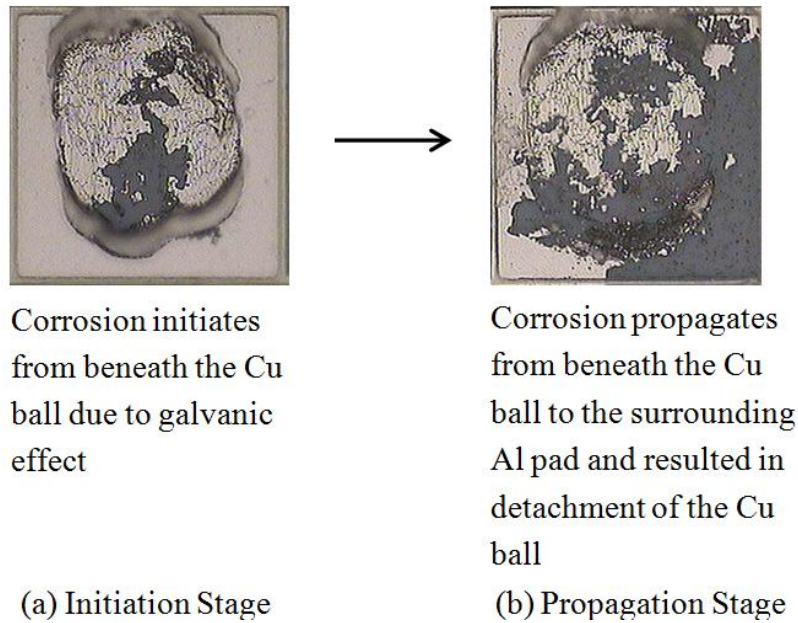


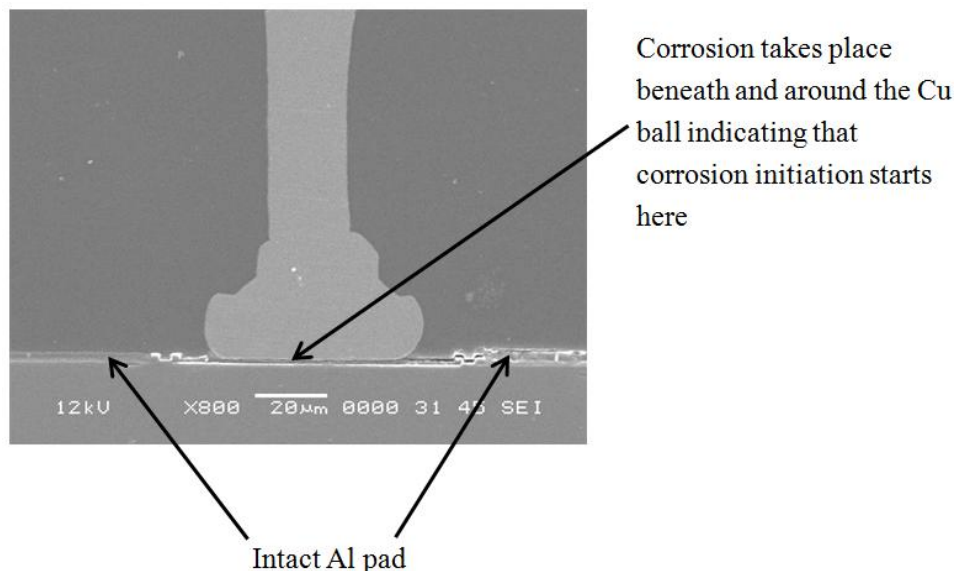
Figure 4 shows the mechanism of galvanic corrosion between the Cu balls and Al pads, the mechanism of initiation is very similar to Au balls, except that Cu intermetallics were not present on the Al pad after the Cu ball was sheared off.

Figure 4. Corrosion mechanism of Cu balls and Al pads at (a) initiation and (b) propagation stage at 5 min soaking time.



Cross-sectional analysis of the Cu ball on Al pad further confirms that corrosion occurs primarily beneath the Cu balls and does not initiate from the Al pad (Figure 5).

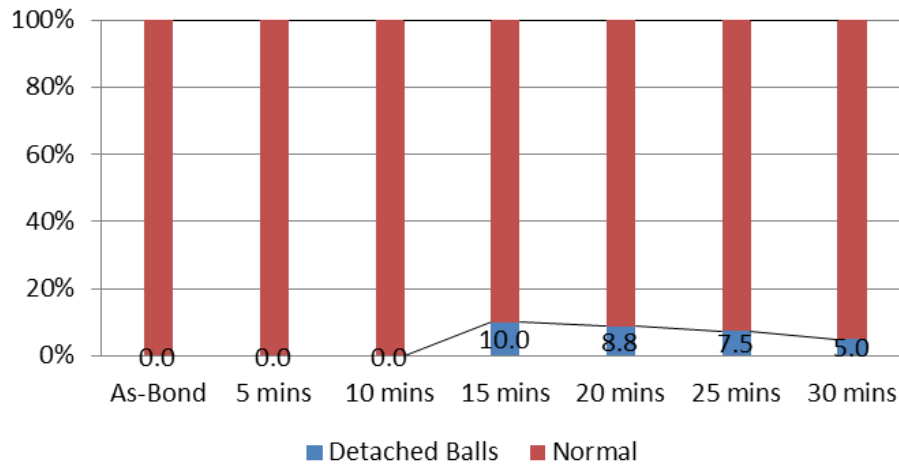
Figure 5. Cross-sectional analysis of Cu ball on Al pad revealing corrosion initiation beneath the Cu ball.



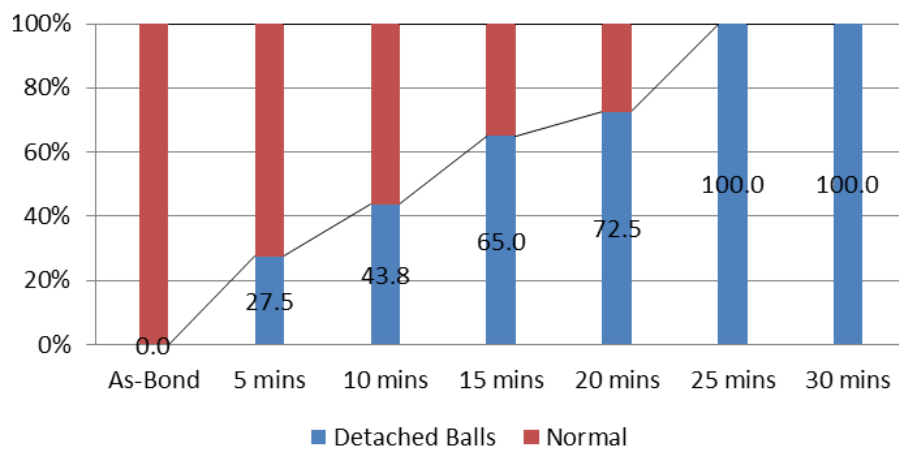
The results on the number of detached balls on Au and Cu wire bonding are shown in Figure 6a,b, respectively. It can be seen from Figure 6a that detachment of Au balls starts only after soaking in

NaCl solution for 15 min. The number of detached balls is also relatively constant, considering that the sample size used is 240 balls, and is kept below 10% even after 30 min. For Cu wire bonding as shown in Figure 6b, the percentage of detached balls increases steadily from 27.5 to 100 within 25 min.

Figure 6. Results on percentage of detached balls on (a) Au and (b) Cu wire bonding.



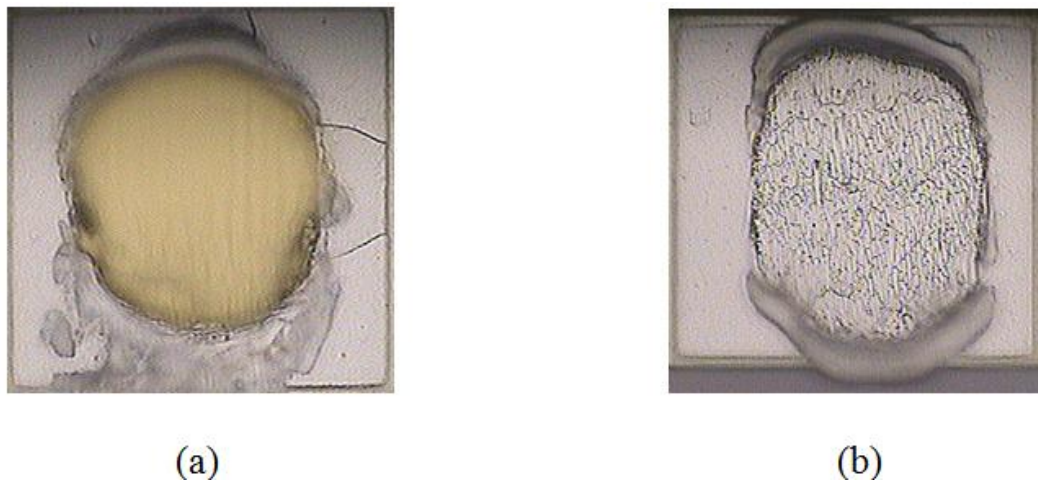
(a)



(b)

According to Figures 3–5, the extensive corrosion at the Al pads and the detachment of the bonded Au and Cu balls is due to galvanic corrosion between Au/Al and Cu/Al. The standard potential difference between Au and Al is 3.2 V, while that of Cu and Al is 2.0 V. Theoretically, there should be more detached Au balls than Cu balls due to the more intense galvanic corrosion in Au/Al wire bonding. However, it was found to be otherwise, as the corrosion of Cu/Al is much more serious than Au/Al. Au is soft, and with the use of thermosonic bonding, good ball pad coverage is obtained due to the intermetallic formation beneath the Au balls. Therefore, Cl^- solution cannot seep in easily to set up the corrosion cell and the corrosion rate is much lower. Figure 7a shows good ball pad coverage for Au after wire bonding. Intermetallic formation is very minimal in Cu/Al at room temperature after wire bonding. Poor ball pad coverage and poor intermetallics are observed for Cu bonding in Figure 7b which allows Cl^- to seep beneath the pad to setup the corrosion cell.

Figure 7. Optical micrographs showing (a) good ball pad coverage with Au intermetallics and (b) very minimal Cu/Al intermetallics.

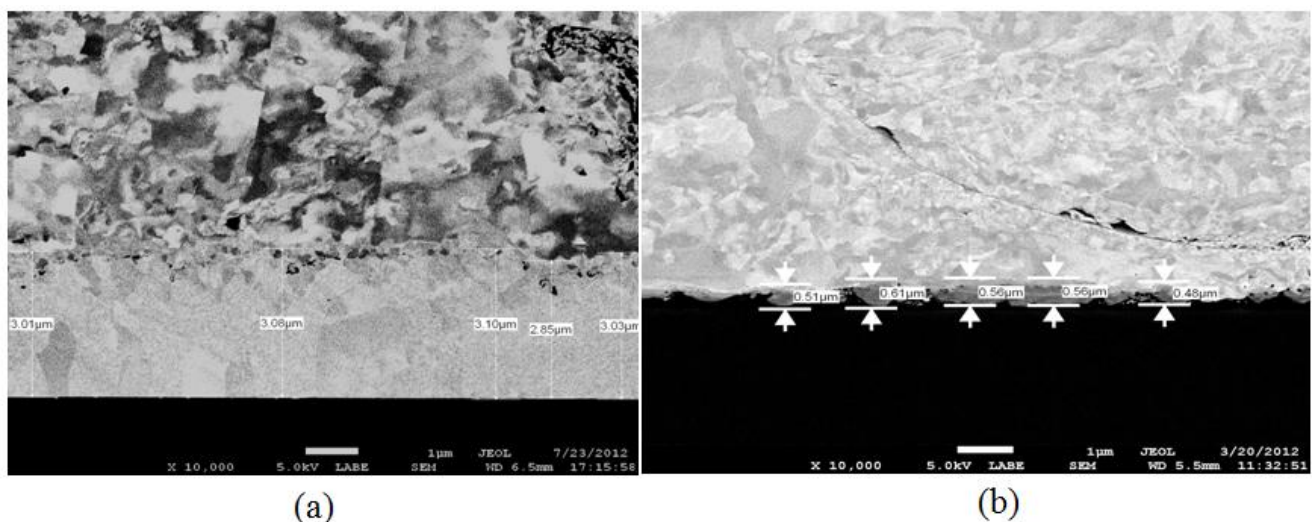


Cu in the presence of Cl^- at pH less than 6 will form CuCl_2^- according to the copper-chlorine Pourbaix diagram [15]. Formation of CuCl_2^- does not allow self-passivation of Cu to occur, and this will inevitably increase the rate of corrosion of Cu. Furthermore, it is known that Cl^- ions can act as a catalyst for Cu corrosion and weakens or dissolves the stable passivation oxide film. The likely intermetallic phases to be corroding in Cu/Al wire bonding would be CuAl and Cu_9Al_4 due to the lower proportion of Al in the intermetallic [12]. In the case of Au/Al wire bonding, Au_4Al was shown to corrode in the presence of Cl^- [16,17].

3.2. Intermetallic Growth Rate Evaluation in Au/Al and Cu/Al Wire Bonding

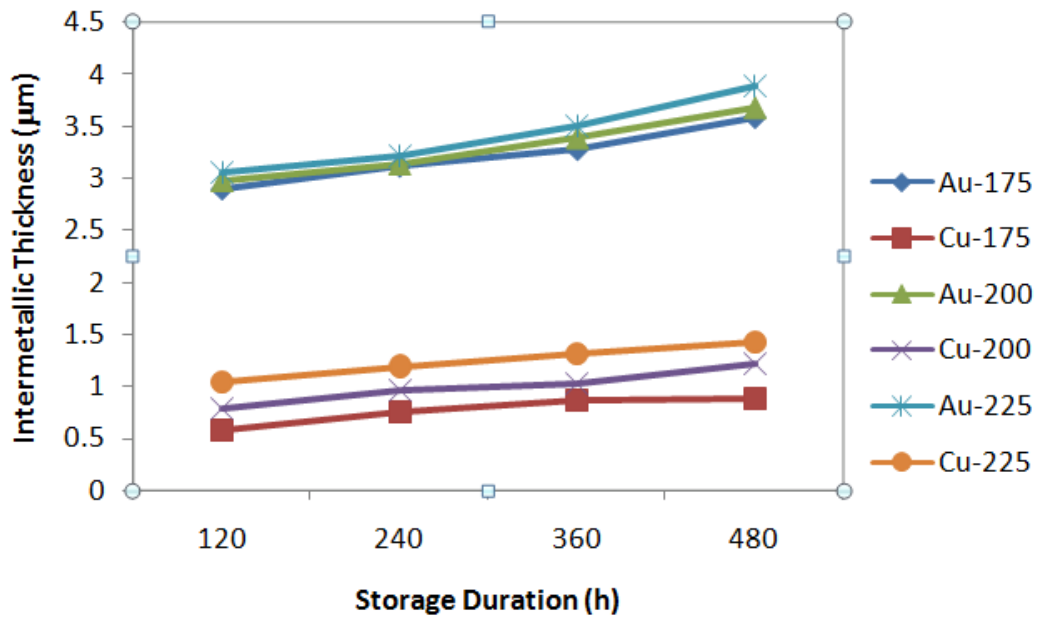
Figure 8 shows a comparison of the intermetallics thickness of Au/Al and Cu/Al wire bonding at the mildest HTS conditions of 175 °C for 120 h. It can be seen from Figure 8a,b that under the same magnification of 10,000 times, the intermetallic layer in Au/Al is about 5 times thicker than Cu/Al.

Figure 8. Intermetallic thickness of (a) Au/Al and (b) Cu/Al wire bonding at HTS conditions of 175 °C for 120 h.



The intermetallics measurement at different storage durations (120 h, 240 h, 360 h and 480 h) and temperatures (175 °C, 200 °C and 225 °C) are shown in Figure 9. As shown in the figure, the intermetallic thickness of Au can range from 3 to 5 times higher than Cu.

Figure 9. Intermetallics measurement at different HTS conditions.



To calculate the intermetallic growth rate and the activation energy for intermetallic formation, the following two Equations [2] are used:

$$X^2 = Kt + K_1 \tag{4}$$

where X = IMC thickness (μm)

t = Annealing time (s)

K = Reaction rate of IMC formation ($\mu\text{m}^2/\text{s}$)

K_1 = Constant related to initial IMC thickness (μm^2)

$$K = K_o e^{(-\Delta Q/RT)} \tag{5}$$

where ΔQ = Activation energy (kcal/mol)

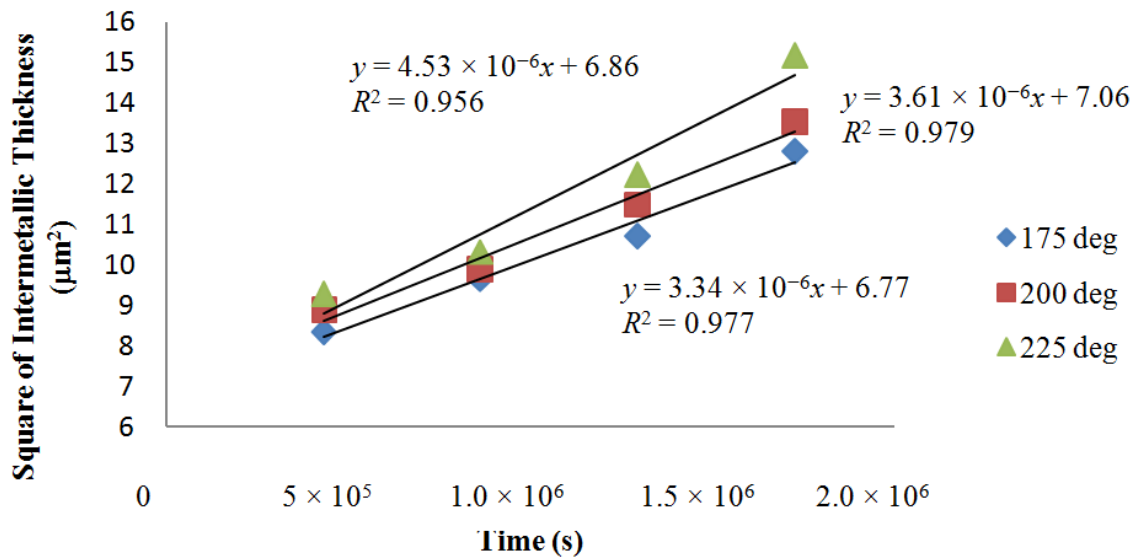
R = Gas constant (1.99 cal/mol K)

T = Annealing Temperature (K)

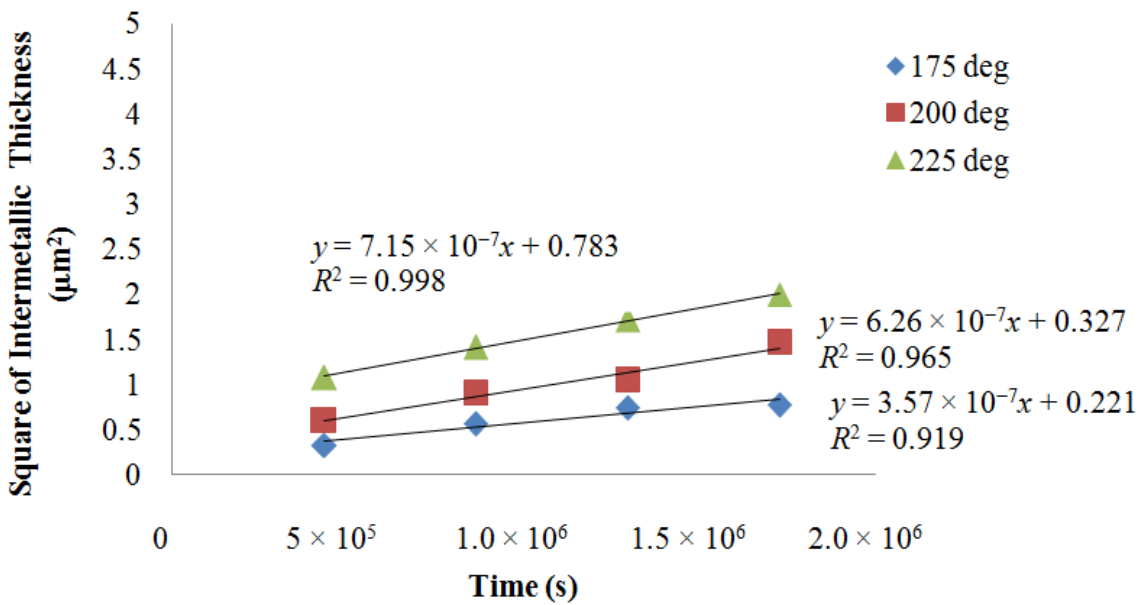
K_o = Pre-exponential Factor ($\mu\text{m}^2/\text{s}$)

Using Equation (4), three graphs of X^2 vs. t is plotted to obtain the gradient K at three different temperatures for Au and Cu wire bonding respectively as shown in Figure 10. K_1 is taken from the average of the three y-intercept values of the three graphs.

Figure 10. Intermetallic growth rates (K) at three different temperatures for (a) Au and (b) Cu wire bonding.



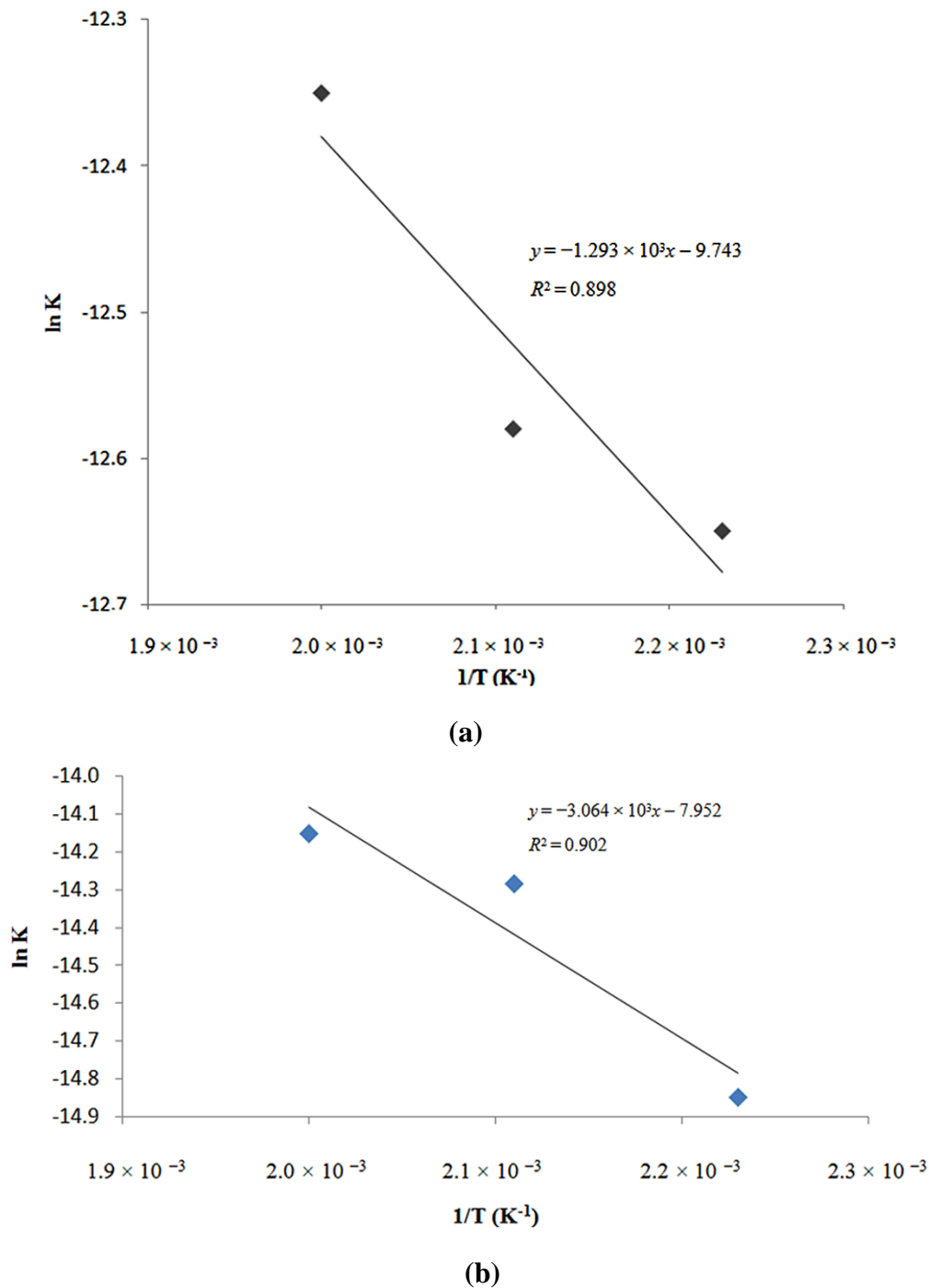
(a)



(b)

Using the K at three different temperatures, graphs of $\ln K$ vs. $1/T$ are plotted for Au and Cu respectively to obtain the activation energy ΔQ (Figure 11). The intermetallic growth rates and the activation energies obtained for both Au and Cu are compared with literature results as shown in Table 4.

Figure 11. Graphs of $\ln K$ vs. $1/T$ are plotted for Au and Cu, respectively, to obtain the activation energy ΔQ .



It can be seen from Table 4 that the rate of intermetallic formation and the activation energies of Au/Al and Cu/Al in the current study is faster and lower, respectively, than previous works. The Al pad metallization used in previous studies was $0.6 \mu\text{m}$ thick, while the pad used in the current work is $1.2 \mu\text{m}$ thick. The thin Al metallization in previous works could be the rate-determining step in preventing faster intermetallic formation and resulted in higher activation energy calculated since the thinnest intermetallic layer that is formed in Cu/Al at the mildest HTS condition is already $0.58 \mu\text{m}$. At more stringent HTS conditions, the intermetallic layers formed are even thicker. The reported and

detectable intermetallic phases in Cu/Al are mainly CuAl₂, CuAl and Cu₉Al₄ [18,19]. Depending on the proportion of these three phases, the Al-rich intermetallics may have difficulties in forming due to a deficit of Al, and resulted in a slower growth rate and higher activation energy. Similarly for Au/Al wire bonding, Al-rich intermetallic phases such as AuAl₂, may have difficulties in forming due to the smaller amount of Al available, especially when the Au intermetallics can grow above 3.8 μm at stringent HTS conditions.

Table 4. Comparison of intermetallic growth rates and activation energies for Au/Al and Cu/Al.

Sample	Author	Time (h)	Temperature (°C)	Rate (μm ² /s)	ΔQ (kcal/mol)
Au	Current	120, 240, 360, 480	175	3.34 × 10 ⁻⁶	2.5
		120, 240, 360, 480	200	3.61 × 10 ⁻⁶	
		120, 240, 360, 480	225	4.53 × 10 ⁻⁶	
	[3]	2, 25, 75, 100, 300	150	1.10 × 10 ⁻¹⁴	–
		2, 25, 75, 100, 300	280	2.40 × 10 ⁻¹¹	
		2, 25, 75, 100, 300	350	3.90 × 10 ⁻¹⁰	
Cu	Current	120, 240, 360, 480	175	3.57 × 10 ⁻⁷	6.1
		120, 240, 360, 480	200	6.26 × 10 ⁻⁷	
		120, 240, 360, 480	225	7.15 × 10 ⁻⁷	
	[3]	2, 25, 75, 100, 300	150	1.88 × 10 ⁻¹⁶	26
		2, 25, 75, 100, 300	250	2.64 × 10 ⁻¹³	
		2, 25, 75, 100, 300	300	3.75 × 10 ⁻¹²	
[6]	100, 250, 500, 1000	150	2.15 × 10 ⁻⁸	10.71	
	100, 250, 500, 1000	200	2.56 × 10 ⁻⁸		
	100, 250, 500, 1000	250	1.08 × 10 ⁻⁷		

The derived intermetallic growth rate equations for Au/Al and Cu/Al in this work are shown respectively in Equations (6) and (7):

$$X^2 = 5.86 \times 10^{-5} e^{(-12935/T)} t + 6.9 \times 10^{-12} \quad (6)$$

$$X^2 = 3.52 \times 10^{-4} e^{(-30645/T)} t + 4.4 \times 10^{-13} \quad (7)$$

4. Conclusions

The following conclusions can be drawn from this study:

- (1) Uniform pitting corrosion occurs on the Al pad in the absence of wire bonding.
- (2) The good Au coverage and intermetallic formation beneath the Au balls strengthens the bonding between Au and Al. Therefore, Cl⁻ solution is not able to seep in easily to set up the corrosion cell, and the corrosion rate in Au/Al is much lower than Cu/Al.
- (3) The intermetallic thickness of Au/Al can range from 3 to 5 times higher than Cu/Al.
- (4) The thin Al metallization in previous works could be the rate-determining step in preventing faster intermetallic formation, and resulted in higher activation energy than what was observed in the current work.

Acknowledgments

The authors would like to thank the World Gold Council for funding this work which is part of a project to understand the limitations of gold and copper ball bond reliability.

Conflict of Interest

The authors declare no conflict of interest.

References

1. Harmon, G. *Wire Bonding in Microelectronics: Materials, Processes, Reliability and Yield*, 2nd ed.; McGraw-Hill: New York, NY, USA, 1997.
2. England, L.; Jiang, T. Reliability of Cu Wire Bonding to Al Metallization. In Proceedings of IEEE Electronic Component Technology Conference, Reno, NV, USA, 29 May 2007; p. 1604.
3. Kim, H.J.; Lee, J.Y.; Paik, K.W.; Koh, K.W.; Won, J.H.; Choe, S.; Lee, J.; Moon, J.T.; Park, Y.J. Effects of Cu/Al intermetallic compound (IMC) on copper wire and aluminum pad bondability. *IEEE Trans. Compon. Packag. Technol.* **2003**, *26*, 367–374.
4. Kurtz, J.; Cousens, D.; Dufour, M. Copper wire ball bonding. In Proceedings of the 34th Electron Component Conference, New Orleans, LA, USA, 14–16 May 1984; pp. 1–5.
5. Mori, S.; Yoshida, H.; Uchiyama, N. The development of new copper ball bonding wire. In Proceedings of the 38th Electron Component Conference, Los Angeles, CA, USA, 9–11 May 1988; pp. 539–545.
6. Na, S.H.; Hwang, T.Y.; Park, J.S.; Kim, J.Y.; Yoo, H.Y.; Lee, C.H. Characterization of intermetallic compound (IMC) growth in Cu wire ball bonding on Al pad metallization. In Proceedings of the 61st Electronic Components and Technology Conference, Lake Buena Vista, FL, USA, 31 May–3 June 2011; pp. 1740–1745.
7. Murali, S.; Srikanth, N.; Vath, C.J. Grains, deformation substructures and slip bands observed in thermosonic copper ball bonding. *Mater. Charact.* **2003**, *50*, 39–50.
8. Nguyen, L.T.; McDonald, D.; Danker, A.R.; Ng, P. Optimization of copper wire bonding on Al-Cu metallization. *IEEE Trans. Compon. Packag. Manufact. Technol. Part A.* **1995**, *18*, 423–429.
9. Tan, C.W.; Daud, A.R.; Yarmo, M.A. Corrosion study at the Cu-Al interface in microelectronics packaging. *Appl. Surf. Sci.* **2002**, *191*, 67–73.
10. Hang, C.J.; Wang, C.Q.; Mayer, M.; Tian, Y.H.; Zhou, Y.; Wang, H.H. Growth behaviour of Cu/Al intermetallic compounds and cracks in copper ball bonds during isothermal aging. *Microelectron. Reliab.* **2008**, *48*, 416–424.
11. Lee, C.C.; Higgins, L.M. Challenges of Cu wire bonding on low-k/Cu wafers with BOA structures. In Proceedings of the 60th Electronic Components and Technology Conference, Las Vegas, NV, USA, 1–4 June 2010; pp. 342–349.

12. Boettcher, T.; Rother, M.; Liedtke, S.; Ulrich, M.; Bollmann, M.; Pinkernelle, A.; Gruber, D.; Funke, H.-J.; Kaiser, M.; Lee, K.; *et al.* On the intermetallic corrosion of Cu-Al wire bonds. In proceedings of the 12th Electronics Packaging Technology Conference, Singapore, 8–10 December 2010; pp. 585–590.
13. Facility for the Analysis of Chemical Thermodynamics. Available online: <http://www.crct.polymtl.ca/factweb.php> (accessed on 18 March 2013).
14. Foley, R.T.; Hguyen, I.H. The chemical nature of Al corrosion—V. Energy transfer in Al dissolution. *J. Electrochem. Soc.* **1982**, *192*, 464–467.
15. Beverskog, B.; Puigdomenech, I. SKI Rapport 98:19. Pourbaix diagrams for the system copper-chlorine at 5–100 °C. Available online: http://www.stralsakerhetsmyndigheten.se/global/publikationer/ski_import/010803/04318226039/98-19.pdf (accessed on 18 March 2013).
16. Lue, M.H.; Huang, C.T.; Huang, S.T.; Hsieh, K.C. Bromine and chlorine induced degradation of the Au–Al bonds. *J. Electron. Mater.* **2004**, *33*, 1111–1117.
17. Schrapler, L.; Muller, T.; Knoll, H.; Petzold, M. Influence of intermetallic phases on bonding reliability in thermosonic Au–Al wire bonding. In Proceedings of the 1st Electronic System Integration Technology Conference, Dresden, Germany, 5–7 September 2006; pp. 1266–1273.
18. Rajan, K.; Wallach, E.R. A transmission electron microscopy study of intermetallic formation in Al-Cu thin film couples. *J. Cryst. Growth* **1980**, *49*, 297–302.
19. Tamou, Y.; Li, J.; Russell, S.W.; Mayer, J.W. Thermal and ion beam induced thin film reactions in Cu-Al bilayers. *Nucl. Instrum. Methods Phys. Res. B* **1992**, *64*, 130–133.

© 2013 by the authors; licensee MDPI, Basel, Switzerland. This article is an open access article distributed under the terms and conditions of the Creative Commons Attribution license (<http://creativecommons.org/licenses/by/3.0/>).